



POLITECNICO DI TORINO  
Repository ISTITUZIONALE

Dynamic Analysis Of Rotors: Comparison Between the Simplified One-Dimensional Results and Those Obtained Through 3-D Modeling

*Original*

Dynamic Analysis Of Rotors: Comparison Between the Simplified One-Dimensional Results and Those Obtained Through 3-D Modeling / G. Genta; M. Silvagni; C. Qingwen. - STAMPA. - (2013). ((Intervento presentato al convegno XXI Congresso nazionale AIMETA tenutosi a Torino nel September 2013.

*Availability:*

This version is available at: 11583/2526352 since:

*Publisher:*

*Published*

DOI:

*Terms of use:*

openAccess

This article is made available under terms and conditions as specified in the corresponding bibliographic description in the repository

*Publisher copyright*

(Article begins on next page)

# Dynamic analysis of rotors: comparison between the simplified one-dimensional results and those obtained through 3-D modeling

Giancarlo Genta<sup>1</sup>, Mario Silvagni<sup>1</sup>, Cui Qingwen<sup>1</sup>

<sup>1</sup>*Department of Mechanical and Aerospace Engineering, Politecnico di Torino, Italy*  
*E-mail: giancarlo.genta@polito.it, mario.silvagni @polito.it*

*Keywords:* Rotordynamics, FEM, solid modeling.

**SUMMARY.** Three-dimensional FEM modeling is a viable alternative to simpler approaches also in rotordynamic analysis. However, some difficulties are still present, and not all commercial codes are able to deal with this kind of modeling in an adequate way. In the day-to-day industrial practice there is some concern related to the use of 3-D modeling, even if it has the huge advantage of being better integrated into the Computer Aided Engineering (CAE) practices that lead to a decrease of the design and analysis costs and times. The present paper aims to shed some light on the improvements in the quality of the analysis results achievable through 3-D modeling in rotordynamics: since there is no chance of obtaining general results in this field, the task will be carried on by proceeding with numerical experiments related to hundreds of different cases, that are by necessity much simplified, but are emblematic of the actual rotor configurations.

## 1 INTRODUCTION

The traditional approach to rotordynamic analysis is based on modeling rotor shafts as beams and elements like discs, joints, gearwheels, etc. as concentrated masses, often provided with moments of inertia. This approach is usually referred to as one-dimensional (1-D) modeling. The models based on it may have different complexity, spanning from elementary 2 degrees of freedom models (the Jeffcott rotor), to models with 4 d.o.f. up to general multi d.o.f. models based either on the transfer matrices approach of the Finite Elements Method (FEM) [1-4].

The limitations of 1-D rotordynamics are mainly two:

1. The first drawback is linked with the beam-like nature of the shafts. It is well known that the Euler-Bernoulli model can be used only for fairly slender beams and that even the Timoshenko beam cannot model correctly beams with a too low slenderness. Moreover, the rotors of many turbines include tubular shafts with large diameter and small thickness, and in this case the natural frequencies linked with bending in the circumferential direction, not obtained using beam models, may lay in the same range as those linked with bending in the axial direction. A similar effect is linked to some rotor configurations that can be assimilated more to drums than to shafts.
2. The second limitation of 1-D rotordynamics is the impossibility of accounting for the flexibility of discs, that may, in some cases, affect the dynamic behavior of actual rotors. This can be corrected by resorting to the so-called 1 1/2-D approach, in which the discs are modeled using annular elements whose displacements are developed in Fourier series along the angle. The main drawback of this approach is that of being limited to thin discs having an overall axy-symmetrical shape. The advantage is that the model is only marginally more complicated than that obtained through the 1-D approach [5, 6].

Although it is possible to show that the modes in which the geometric centers of the cross sections don't displace laterally are uncoupled with the overall rotor modes, these local modes may be important in assessing the global dynamics of the rotor [5-7].

The only way to include all these effects in the analysis is to resort to full three-dimensional (3-D) modeling of the rotor, a thing that is made possible by using the FEM. Even if the basic foundations of 3-D rotordynamics were defined since a long time [8], the application of 3-D modeling of rotors is not as easy as it could be expected, since not all commercial FEM codes are suitable for rotor modeling, and those which are, acquired this capability only recently. A problem that can be encountered in 3-D rotor modeling is linked with the symmetry classes of the rotor: the analysis should be performed with reference to an inertial frame if the rotor is axially symmetrical, while a rotor-fixed frame must be used if the rotor is not such, provided that the stator has axial symmetry. If both rotor and stator have no symmetry axis, an equation of motion with time-dependent coefficients is obtained in any reference frame and no closed form solution can be obtained.

Actually the axial symmetry of both stator and rotor are not strictly required, since it may be substituted by the simpler cyclic symmetry, but in this case a modal computation must be performed [9].

It must be expressly stated that the greatest advantage of 3-D rotordynamics is not so much in the results it allows to obtain but on its compatibility with the models that must be anyway built in the overall Computer Aided Engineering (CAE) process. A 3-D model of the rotor and often of the whole machine must anyway be made, while a beam model, like the one required for the simpler approaches to rotordynamics, has to be expressly built through specific, labor intensive, computations, since the conversion is not easily automated. The building of 1-D, and even more 1 1/2-D, models requires more common sense and engineering knowledge than the application of algorithms, a thing that rules out a simple automatization of the procedure.

This notwithstanding, industrial applications of 3-D rotordynamics are still less common than what could be thought, and ad hoc, 1-D, and even 1 1/2-D rotordynamic codes still find a widespread application.

The aim of the present paper is to evaluate, through a number of examples, how accurate are the results of the simple 1-D and 1 1/2-D models when compared with complex 3-D models even in conditions that usually are considered beyond the applicability of the simplified models. This comparison is based on a simplified geometry, usually referred to as *Stodola-Green rotor*.

## 2 THE STODOLA-GREEN ROTOR

The Stodola-Green rotor is made of a rotating cantilever beam to which a rigid body is attached. In its simplest (Fig. 1a) form the shaft is prismatic and homogeneous and the rigid body is a constant thickness axi-symmetric disc. By varying the characteristics of the beam it is possible to investigate on the adequateness of the beam model (point (1) above), while by varying the thickness of the disc it is possible to investigate on the effects of the disc flexibility (point (2) above).

If the two parts are made with the same material, the geometry is defined by 5 parameters ( $l_b$ ,  $d_b$ ,  $d_o$ ,  $l$  and  $d$ ) and the material properties by 3 parameters ( $E$ ,  $\nu$  and  $\rho$ ).

The simplest model allowing to take into account gyroscopic effects, i.e. the rotor with 4 degrees of freedom (Fig. 1b), yields the following eigenproblem allowing to compute the Campbell diagram, i.e. the plot of the whirl frequencies as functions of the rotational speed:

$$\det \left( -\omega^2 \begin{bmatrix} m & 0 \\ 0 & J_t \end{bmatrix} + \omega \Omega^2 \begin{bmatrix} 0 & 0 \\ 0 & J_p \end{bmatrix} + K \right) = 0 \quad (1)$$

The parameters included in Eq. (1) are

$$m = \frac{\pi}{4} d^2 l \rho, \quad J_p = m \frac{d^2}{8}, \quad J_t = \frac{m}{4} \left( \frac{d^2}{4} - \frac{l^2}{3} \right) \quad (2)$$

Using the Timoshenko beam model for the part AB of the beam in Fig. 1b and assuming that the length BG is rigid, the stiffness matrix is

$$\mathbf{K} = \frac{EI}{l_b^3 (1 + \phi)} \begin{bmatrix} 12 & -6(l_b + l) \\ -6(l_b + l) & l_b^2 (4 + \phi) + 6l_b l + 3l^2 \end{bmatrix} \quad (3)$$

where

$$I = \frac{\pi}{64} (d_o^4 - d_i^4), \quad \phi = \frac{12 EI \chi}{GA l_b^3} \quad (4)$$

and the shear factor  $\chi$  takes a value of 10/9 in the case of circular or annular cross section.

The case of the Euler-Bernoulli beam can be studied by simply assuming that  $\phi = 0$ .

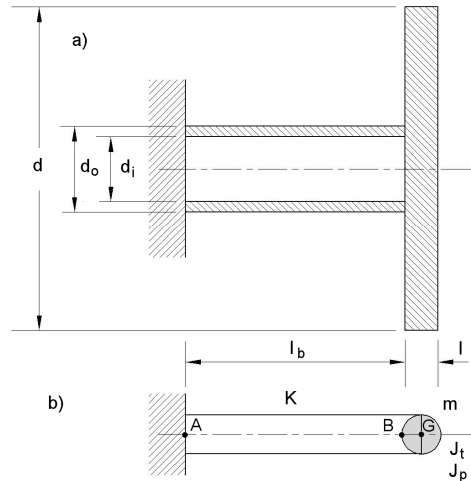


Figure 1: a): Sketch of a Stodola-Green rotor; b): model as a rotor with 4 d.o.f.

The Stodola-Green rotor is studied using 10 different models:

1. Model 4-DOF-EB: a simplified 4 degrees of freedom model, with an Euler Bernoulli beam (Eq. (1) to (3));
2. Model 4-DOF-T: a simplified 4 degrees of freedom model, with a Timoshenko beam;
3. Model 1D-ML: a 1-D FEM model, built using the DYNROT code. The model is made by 4 Timoshenko beam models for the shaft and 2 similar beam elements for the disc (equivalent to a rigid beam plus a mass element). The beam is massless;
4. Model 1D-M: identical to Model 1D-ML, but with the mass of the beam accounted for;

5. Model 1.5D-ML: a 1 1/2-D FEM model, built using the DYNROT code. The model is made by 6 Timoshenko beam for the shaft, 1 disc-shaft transition model and 3 disc elements for the disc. The 4 elements modeling the beam are massless.
6. Model 1.5D-M: identical to Model 1.5D-ML, but with the mass of the beam accounted for;
7. Model 1D-A-ML: a 1-D FEM model built using ANSYS code. The same type and number of elements as for the DYNROT model. The mass of the beam is neglected;
8. Model 1D-A-M: identical to Model 1D-A-ML, but the mass of the beam is accounted for.
9. Model 3D-A-ML: a 3-D FEM model built using ANSYS code. This model is much more complex than the previous ones. It is made by a variable number of type 272, general axisymmetric 3-D solid models, with 4 nodes. The number of elements depends on the dimensions of the various parts, so that the elements are not too distorted. The beam is massless.
10. Model 3D-A-M: identical to Model 3D-A-ML, but the mass of the beam is accounted for.

### 3 EFFECT OF THE SLENDERNESS OF THE SOLID BEAM

To study the effect of the slenderness of the beam, 4 geometrical parameters are fixed ( $l_b$ ,  $d_i$ ,  $l$  and  $d$ ), together with the properties of the material, while the outer diameter of the beam  $d_o$  is considered as a variable.

Assume that  $l_b = 500$  mm,  $d_i = 0$ ,  $l = 100$  mm,  $d = 500$  mm,  $E = 210$  GPa,  $\rho = 7810$  kg/m<sup>3</sup>,  $\nu = 0.3$  and that the outer diameter is varied between 20 mm (very slender beam) to 400 mm (very stub beam, practically not a beam but a solid).

Since the problem here is linked only with the stiffness of the system, the beam is assumed to be massless, so that it is possible to compare the FEM results also with those obtained using the 4 d.o.f. model. In this way a comparison between the Euler-Bernoulli and the Timoshenko beam elements is also possible. The thickness of the disc is large, and no effects of disc flexibility can be expected: the 1-D and the 1 1/2 D models are expected to give the same results.

#### 3.1 First critical speed

The dynamic study is performed using models # 1 (4-DOF-EB), # 2 (4-DOF-T), #3 (1D-ML), #5 (Model 1.5D-ML), #7 (1D-A-ML) and #9 (3D-A-ML). The results, in terms of the first critical speed, are shown in Fig. 2, a to c.

The critical speed is reported as a function of the beam diameter in Fig. 2a. The part for very small diameters is enlarged by a factor 10 to allow the results to be seen clearly. The results for stub beams are reported as functions of the slenderness in Fig. 2b. The Slenderness is defined as

$$\alpha = \frac{l_b \sqrt{A}}{\sqrt{I}} \quad (4)$$

In Fig. 2c the ratio between the critical speed  $\Omega_{\text{crit}}$  computed with the current model and that resulting from the Euler-Bernoulli model  $\Omega_{\text{crit}}^*$  are reported as a function of the slenderness.

The results are clear: the 1-D, 1 1/2-D and 3-D models yield very similar results. The largest difference between the 1-D and 3-D elements occurs at a slenderness of 5, where the relative error between the first two models and the latter one is of 1.5%, to reduce below 1% for a slenderness greater than 10. The Timoshenko beam model is successful in predicting the behavior of the beam even for a slenderness as small as 5.

The value of the first critical speed (in rad/s) is reported for different values of the slenderness of the beam, computed with the various models in Tab. 1.

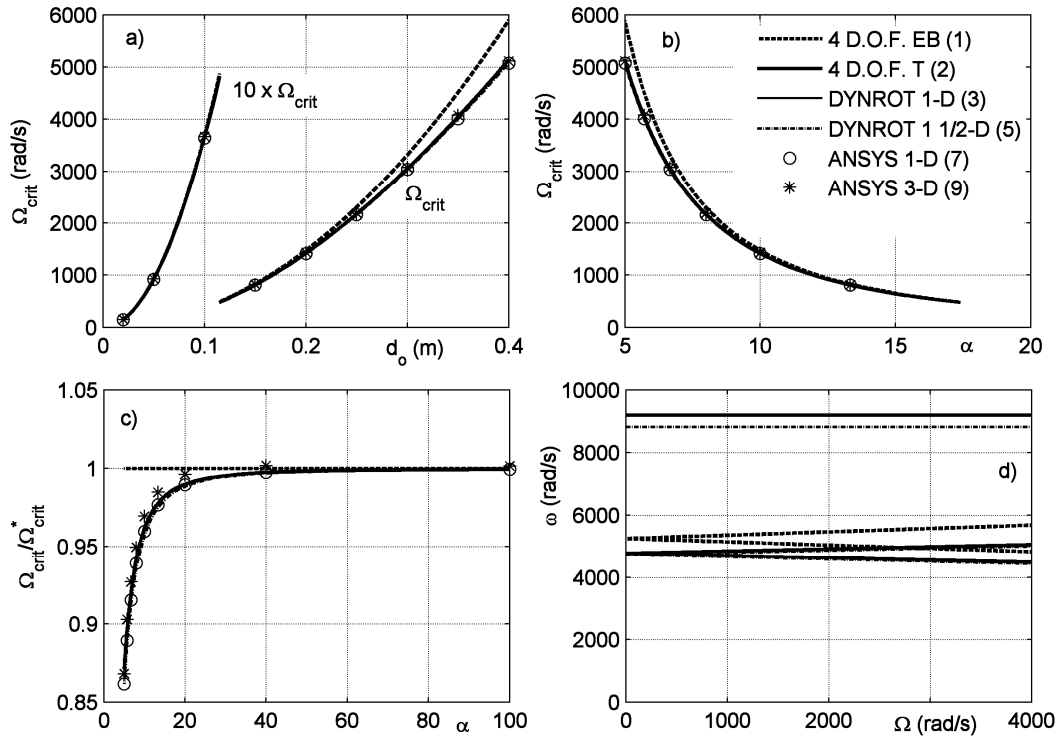


Figure 2: a): Critical speed as a function of the beam diameter (The part on the left, for very small diameters, is enlarged by a factor 10); b): Critical speed as a function of the slenderness for very stub beams; c): ratio between the critical speed  $\Omega_{crit}$  computed with the current model and that resulting from the Euler-Bernoulli model  $\Omega_{crit}^*$  as a function of the slenderness; d): Campbell diagram for the rotor with  $d_0 = 400$  mm (first bending and torsional modes).

Tab. 1. First critical speed (in rad/s) for different values of the slenderness  $\alpha$  of the beam, computed with the various models.

$\alpha$	5	10	20	40	100
4 d.o.f. – Euler-Bernoulli	5,892	1,473	368.2	92.1	14.7
4 d.o.f. – Timoshenko	5,134	1,417	364.6	91.8	14.7
DYNROT 1-D	5,125	1,416	364.5	91.8	14.7
DYNROT 1 1/2-D	5,078	1,410	364.0	91.8	14.7
ANSYS 1D	5,077	1,414	364.4	91.8	14.7
ANSYS 3D	5,114	1,428	366.8	92.2	14.7

### 3.2 Campbell diagram

The Campbell diagram for the rotor with  $d_0 = 400$  mm was computed using the same models as for the critical speed. The first bending and the first torsional modes are reported in Fig. 2d as functions of the speed.

The results for the bending mode for models # 2 (4-DOF-T), #3 (1D-ML), #5 (Model 1.5D-ML) are completely superimposed, while the Euler-Bernoulli beam (model # 1 (4-DOF-EB)) gives,

as expected, slightly different results. Note that in the case of the torsional mode the 1 1/2-D model yields a value of the frequency that is slightly lower than that of the 1-D model. This can be explained by the very high torsional stiffness of the beam, that is not much higher than that of the disc.

#### 4 EFFECT OF THE THICKNESS OF THE HOLLOW BEAM

The shafts of many turbines are large diameter, thin walled tubes. In these conditions it is often said that beam models are inadequate, owing to the deformations in radial direction of the structure, that follow a multi-lobe pattern. Clearly they cannot take into account these modes, which however are usually local modes and do not affect the rotor as a whole.

To study the effect of the wall thickness of the beam, 4 geometrical parameters are fixed ( $l_b$ ,  $d_o$ ,  $l$  and  $d$ ), together with the properties of the material, while the inner diameter of the beam  $d_i$  is considered as a variable.

Assume that  $l_b = 500$  mm,  $d_o = 400$  mm,  $l = 100$  mm,  $d = 500$  mm,  $E = 210$  GPa,  $\rho = 7810$  kg/m<sup>3</sup>,  $\nu = 0.3$  and the inner diameter is varied between 300 mm (very thick wall beam) to 399 mm (very thin 0.5 mm wall). The slenderness is very low in all cases, so low that the applicability of beam models might be questionable.

In the present case the beam is not assumed to be massless, since the local vibrations are strictly linked with the mass property of the beam and not those of the disc. However, to compare the results with those of the model with 4 d.o.f., also the massless case is considered. The dynamic behavior has been computed using all models, from # 1 to #10.

##### 4.1 First critical speed

The results are reported in Fig. 3.

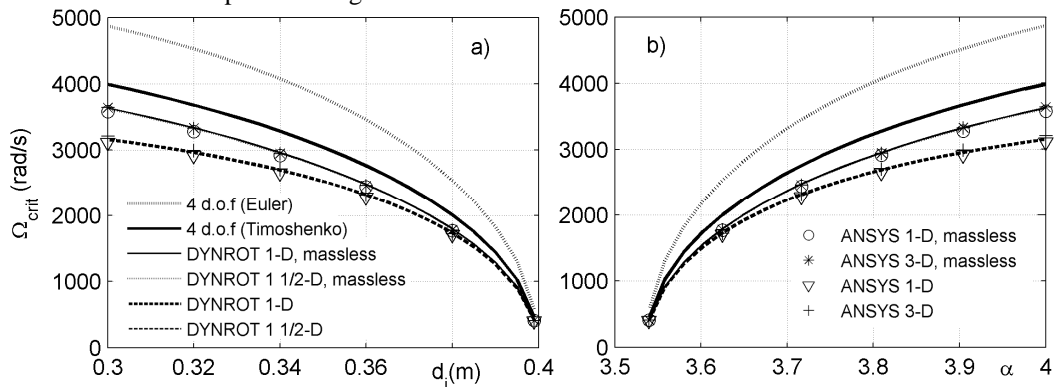


Figure 3: a): Critical speed as a function of the inner diameter of the beam; b) Critical speed as a function of the slenderness.

Owing to the low slenderness, the Euler Bernoulli beam gives results far higher than those due to the Timoshenko beam (owing to neglecting the shear compliance, the beam is way too stiff, relative error between 35% and 45%). The mass of the beam affects the results to a lesser, although noticeable, extent. However, the difference between the results obtained for all wall thicknesses down to just 0.5 mm (thickness/diameter ratio of 0.00125, slenderness of 3.54) is of about 1.5% between the DYNROT model and the ANSYS 3D model.

#### 4.2 Campbell diagram

The Campbell diagram is computed only for the case with the minimum thickness, 0.5 mm (slenderness of 3.55). The results are shown in Fig. 4.

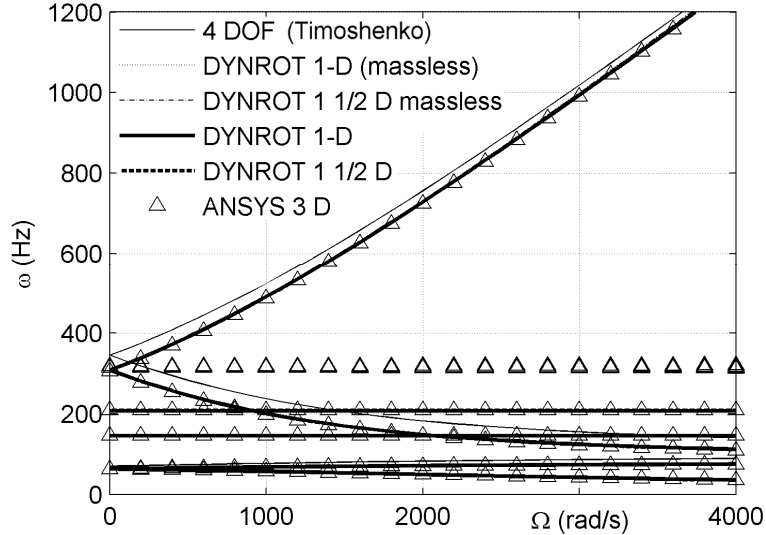


Figure 4 Campbell diagram for the Stodola-Green rotor with a very thin walled beam. The natural frequencies at zero speed computed using the same models are reported in Tab. 1.

Tab. 1. Natural frequencies (in Hz) at zero speed, computed with the various models.

Multiplicity	Bending		Axial	Torsional	2	2
	2	2	1	1		
4 d.o.f. – Euler-Bernoulli	83.51	561.66	208.65	146.22	-	-
4 d.o.f. – Timoshenko	69.92	345.66	208.65	146.22	-	-
DYNROT 1-D (massless)	63.41	310.04	208.65	146.21	-	-
DYNROT 1(1/2)-D (massl.)	63.41	309.82	208.61	146.15	-	-
DYNROT 1-D	63.28	308.31	208.97	145.72	-	-
DYNROT 1(1/2)-D	63.28	308.11	208.06	145.66	-	-
ANSYS 3D	62.66	304.88	208.30	145.62	314.31	317.36

The results are quite close to each other. It is remarkable that the results obtained using the Timoshenko beam are so good (in case of the first mode) even with a slenderness of only 3.55. The worst results for the second mode can be ascribed to the fact that the mass of the beam has been neglected in the 4 d.o.f. model. The 2 higher modes obtained from the 3-D FEM model are due to multilobe deformations.

#### 5 EFFECT OF THE THICKNESS OF THE DISC

To investigate on the effect of the disc thickness on the dynamics of the Stodola-Green rotor the 4 geometrical parameters that are fixed are  $l_b$ ,  $d_o$ ,  $d_i$ , and  $d$ , together with the properties of the material, while the disc thickness is considered as a variable.

Assume that  $l_b = 500$  mm,  $d_i = 0$ ,  $d_o = 50$  mm,  $d = 500$  mm,  $E = 210$  GPa,  $\rho = 7810$  kg/m<sup>3</sup>,  $\nu = 0.3$ . The disc length is varied between 100 mm (very thick disc) to 0.5 mm (the disc is practically a



membrane. The slenderness of the beam is high enough ( $\alpha = 40$ ) to expect that the Euler Bernoulli beam is adequate.

### 5.1 First critical speed

The first critical speed is thus computed using all models. The results are reported in Fig. 5.

The results obtained from all models are very similar, except when the disc is very thin (less than 10 mm, i.e.  $l/d < 0.02$ ) and the mass of the shaft becomes an important part of the total mass (therefore the massless models yield results much different from those of the models including the shaft mass). Centrifugal stiffening has a small effect and 1-D, 1 1/2-D and 3-D models yields practically identical results since the frequency of the modes related to the disc deformations grow fast with the speed, remaining well above the  $\omega = \Omega$  line. They do not affect critical speeds.

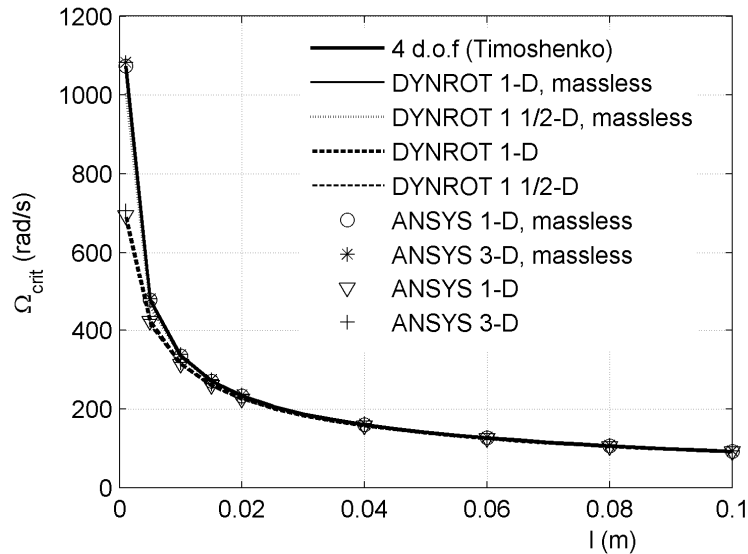


Figure 5. Critical speed as a function of the thickness of the disc.

### 5.2. Campbell diagram

The Campbell diagram was then computed for the case with  $l = 10$  mm. The results are reported in Fig. 6. In Tab. 2 the natural frequencies are reported at standstill.

From the plot and the table the following results can be drawn:

- The 1-D FEM model with massless shaft gives results that are very close to those obtainable from the 4 d.o.f. model, with both Timoshenko and Euler Bernoulli beams. The latter yield 6 natural frequencies (at standstill two have a multiplicity of 2), while the former yields more of them, 6 close to those obtained through the 4 d.o.f. model, and the others much higher.
- At zero speed all models give practically coincident results for the first bending mode (forward and backward) and the first torsional mode. In these modes the disc behaves like a rigid body vibrating on a massless shaft.
- For all other modes the flexibility of the disc and the inertia of the shaft are important in determining the frequencies and the mode shapes. The 1-D models consequently are not usable, and the same holds for the 1(1/2)-D models with a massless shaft.

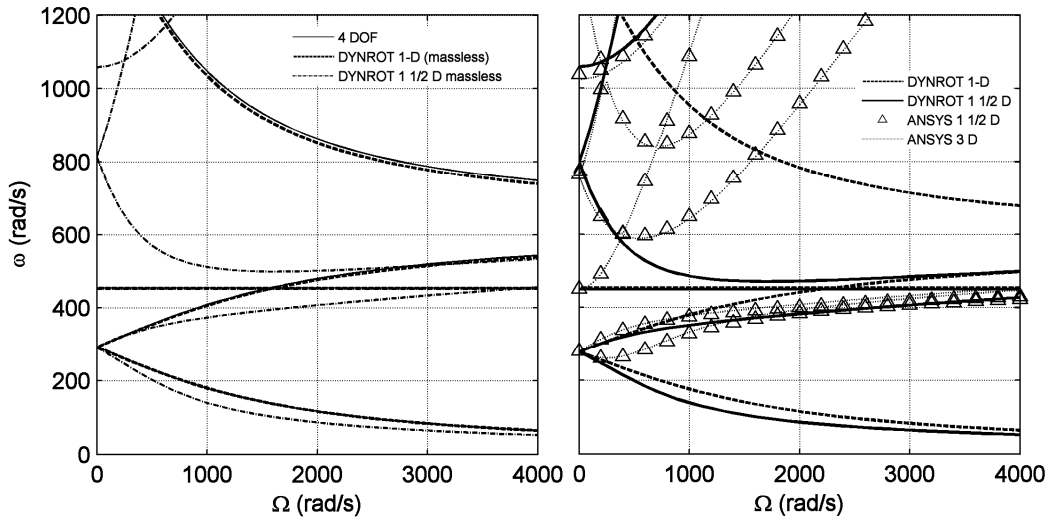


Figure 6. Campbell diagram for the case with  $l = 10$  mm. .

Tab. 2. Natural frequencies (in rad/s) at zero speed, computed with the various models. In the case of ANSYS models also the cases in which the disc is modeled using shell elements are considered. The shaft is modeled either with beam or with solid elements. The first 4 lines refer to models in which the mass of the shaft has been neglected

Multiplicity	Bending			Torsional	Axial
	2	2	2	1	1
4 d.o.f. (Euler-Bernoulli)	292.6	1,591.5	-	454.8	7,333.3
4 d.o.f. (Timoshenko)	292.0	1,577.7	-	454.8	7,333.3
DYNROT 1-D (massless)	292.0	1,577.5	-	454.8	7,333.3
DYNROT 1(1/2)-D (massless)	289.7	812.2	6,355.3	451.1	1,058.2
DYNROT 1-D	278.6	1,459.3	5,959.7	454.4	6,776.1
DYNROT 1(1/2)-D	276.8	796.8	4,124.9	450.7	1,058.2
ANSYS (beam+shell elements)	279.9	766.6	4,190.9	450.4	1,037.4
ANSYS (beam+solid l elements)	274.2	657.8	4,068.0	437.0	969.1
ANSYS (solid+shell l elements)	280.4	722.6	4,153.2	448.0	1,005.3
ANSYS (solid+solid l elements)	281.2	757.9	4,159,6	450.4	1,023.8

- The commercial 1-D FEM code yields results that are practically coincident with those of the DYNROT code, used to produce a 1-D model.
- The results obtained from the ANSYS models (here a model with beam elements for the shaft and shell elements for the disc, ANSYS 1 1/2D, was considered together with the full 3D model, ANSYS 3D) diverge from those obtained using DYNROT at increasing speed. This behavior was unexpected and requires further study. It will be the subject of a future paper.

To clarify the matter, other tests were performed by including only the gyroscopic terms but not centrifugal stiffening. In this case the DYNROT and ANSYS results were practically coincident. This allows to focus further studies on the way centrifugal stiffening is accounted for.

Centrifugal stiffening has some effect even on the first mode; on the other modes these effects are much larger. This consideration is however likely to depend much on the rotor configuration

and may be impossible to generalize it.

## 6 CONCLUSIONS

The simple Stodola-Green rotor here studied allows to draw some considerations about rotor modeling of different complexity, that can have some general applications. The main conclusions are:

- The simplified 4-degrees of freedom models yield good results provided that the mass of the shaft is small when compared with that of the rotor (a fairly obvious conclusion).
- The Euler Bernoulli beam model works well if the slenderness of the beam is high. This may again appear obvious, but it is less obvious that this model is here shown to yield correct results for a slenderness  $\alpha$  as low as 10. The Timoshenko beam model has here been shown to work very well for values of  $\alpha$  as low as 5 and in some cases even 3.5.
- The beam model is able to predict accurately the dynamic behavior of thin walled hollow beams. In this case even a beam with a slenderness of 3.55 and with a thickness/diameter ratio of 0.00125 can be modeled using the 1-D model. Such a thin walled beam has vibration modes that cannot be computed using the 1-D model; however, these modes are uncoupled with the dynamics of the rotor as a whole and can be dealt with as 'local modes'.
- In case the discs are thin, their dynamics cannot be neglected, even if the first bending and torsional modes may be exceptions from this viewpoint. The presence of thin discs makes centrifugal stiffening an important issue, that compels to use the 1 1/2 -D or the 3-D approach. However, the results obtained using the ANSYS code diverge from those obtained using the DYNROT code. This behavior, which apparently is due to the way centrifugal stiffening is accounted for, needs to be clarified and further study is needed. It will be the subject of a future paper.

The above conclusions were drawn from a much simplified model, the Stodola-Green rotor. Some of them can be generalized, but all generalization require care when are based on purely numerical computations. Further studies based on rotor configurations more close to those encountered in applications, and specifically on rotors provided with blades, are needed.

### References

- [1] F.M. Dimentberg, *Flexural Vibrations of Rotating Shafts*, Butterworth, London, 1961
- [2] R.G. Loewi and V.J. Piarulli, *Dynamics of Rotating Shafts*, The Shock and Vibration Information Center, Naval Res. Lab., Washington, D.C., 1969.
- [3] A. Muszyńska, *Rotordynamics*, Springer, CRC Press Boca Raton, 2005.
- [4] G. Genta, *Dynamics of Rotating Systems*, Springer, New York, 2005.
- [5] G. Genta, A. Tonoli, *A Harmonic Finite Element for the Analysis of Flexural, Torsional and Axial Rotordynamic Behaviour of Discs*, Journal of Sound and Vibration, 196(1), 1996, pp. 19-43.
- [6] G. Genta, A. Tonoli, *A Harmonic Finite Element for the Analysis of Flexural, Torsional and Axial Rotordynamic Behaviour of Bladed Arrays*, Journal of Sound and Vibration, 207(5), 1997, pp. 693-720.
- [7] G. Genta, C. Feng, A. Tonoli, *Dynamics behavior of rotating bladed discs: A finite element formulation for the study of second and higher order harmonics*, Journal of Sound and Vibration, Vol. 239, n. 25, Dec. 2010, p. 5289-5306
- [8] M. Gerardin and N. Kill, *A new approach to finite element modelling of flexible rotors*, Engineering Computations, Vol. 1, (1984), 52-64.
- [9] G. Genta and M. Silvagni, *Some Considerations on Cyclic Symmetry in Rotordynamics*, ISCORMA-3, Cleveland, September 2005.